Available online at www.sciencedirect.com

ScienceDirect

Energy Procedia 124 (2017) 379–383

Energy Procedia

www.elsevier.com/locate/procedia

7th International Conference on Silicon Photovoltaics, SiliconPV 2017

ITO-free metallization for interdigitated back contact silicon heterojunction solar cells

Johann-Christoph Stang[a],*, Max-Sebastian Hendrichs[b], Agnes Merkle[c], Robby Peibst[c], Bernd Stannowski[b], Lars Korte[a], Bernd Rech[a]

[a]*Helmholtz-Zentrum Berlin, Institute Silicon Photovoltaics, Kekuléstr. 5, 12489 Berlin, Germany*
[b]*Helmholtz-Zentrum Berlin, PVcomB, Schwarzschildstr. 3, 12489 Berlin, Germany*
[c]*Institute for Solar Energy Research Hameln, 31860 Emmerthal, Germany*

Abstract

We report on two different approaches to fabricate interdigitated back contact silicon heterojunction solar cells without using indium tin oxide (ITO). The standard ITO/Ag backend is either modified by replacing ITO with aluminum-doped zinc oxide (AZO) or completely replaced by a sole aluminum (Al) layer. The very transparent AZO enhances the optical properties at the rear side resulting in an increase in short-circuit current density. The efficiency of the AZO cells remains on the level of the ITO ones, as the fill factor drops slightly. On the contrary, the contact resistivity of annealed Al, in comparison to ITO and AZO, to the emitter and BSF layers is much lower, thus the fill factor is increased. Despite lower open circuit voltages, cells with Al achieve efficiencies of up 22 %, a gain of 0.5 %abs compared to the ITO reference.

Peer review by the scientific conference committee of SiliconPV 2017 under responsibility of PSE AG.

Keywords: silicon heterojunction; back contact; ITO; aluminium; aluminum doped zinc-oxide; metallization

1. Introduction

The amorphous/crystalline (a-Si:H/c-Si) silicon heterojunction technology represents a viable approach to achieve outstanding solar cell efficiencies. The full-area surface passivation by intrinsic amorphous silicon allows for

* Corresponding author. Tel.: +49 30 8062 41356
E-mail address: johann-christoph.stang@helmholtz-berlin.de

1876-6102
Peer review by the scientific conference committee of SiliconPV 2017 under responsibility of PSE AG.
10.1016/j.egypro.2017.09.253

exceptionally high open circuit voltages close to silicon's theoretical limit of 760 mV [1]. Although such a buffer layer potentially hinders current transport at the a-Si:H/c-Si interface, fill factors on the level of conventional diffused junction solar cells have been achieved [2]. In order to maximize light absorption the silicon heterojunction technology can be combined with a back contact architecture. Effectively cutting the contact area in half (and thus doubling the series resistance) by moving all contacts to the rear side of the device, further complicates the challenge to achieve high fill factors. Nevertheless an outstanding efficiency of 26.33 % (with a fill factor of 83.8 %) was recently demonstrated using the silicon heterojunction technology in a back contact architecture [3]. To achieve these high values and overcome both of the aforementioned disadvantages inherent to the BC-SHJ approach, a proper contact design is necessary. The choice of the TCO buffer layer plays a crucial role in fulfilling this task. Indium tin oxide (ITO) is commonly used in standard heterojunction cells – on the front side, its lateral conductivity is necessary to transport charge carriers to the narrow grid fingers of the front metallization. On the rear side, a usually more transparent and less conductive ITO is used to optimize the solar cell's optical properties in the longer wavelengths range. In a back contacted architecture, lateral conductivity is not needed since the rear side is usually almost entirely metallized. With the reduced contact area and decreased TCO conductivity, the now less efficient tunnel-recombination contact between the p-type amorphous silicon emitter layer and the (n-type) ITO represents a strong contribution to the solar cell's overall series resistance. Furthermore, taking the cost efficiency of the solar cell into account, ITO cannot be considered as a particularly inexpensive material. This study therefore evaluates the possibility to replace ITO in back contacted silicon heterojunction solar cells, optimally enhancing both the electrical properties and the manufacturing costs of the solar cell. In the first approach, the whole ITO/Ag stack is replaced with a sole aluminum layer, circumventing the a-Si:H/TCO tunnel-recombination contact issue completely and exchanging silver with a cheaper metal. In a second approach, aluminum-doped zinc oxide (AZO) replaces ITO. AZO has similar properties to ITO, but it is easier to structure by wet chemical approaches and less expensive (although fluctuating, indium and tin prices are usually two respectively one order of magnitude higher than those of zinc and aluminum).

2. Experimental

Interdigitated back contact silicon heterojunction solar cells were built on approximately 280 µm thick n-doped float-zone silicon wafers with a resistivity of 1 – 5 Ωcm. The front side was textured with random pyramids with an alkaline solution, the rear side was polished. For the Al cells, the front side passivation and antireflective coating (ARC), consisting of two SiN_X layers, were deposited by a Roth & Rau SiNA plasma enhanced chemical vapor deposition (PECVD) system. The initial SiN_X layer has a nominal thickness of 10 nm and a refractive index of 2.4, the subsequent layer a nominal thickness of 90 nm and a refractive index of 1.96. The intrinsic hydrogenated amorphous silicon (a-Si:H) passivation on the rear side of the Al wafer was deposited in a 13.56 MHz PECVD system, the following doped amorphous silicon layers in a 60 MHz system, with a thickness of roughly 5 nm for the intrinsic layers and approximately 20 nm for each doped layer. For the ITO and AZO cells, the intrinsic a-Si:H passivation layers on both sides, the front side SiN_X antireflective coating, the rear side p-type a-Si:H and n-type hydrogenated nano-crystalline silicon (nc-Si:H) layers [4] were deposited in an RF PECVD cluster tool manufactured by Applied Materials (AKT1600), with the following thicknesses: 5 nm for the intrinsic a-Si:H passivation layers, 80 nm for the SiN_X ARC, roughly 15 nm for both doped a-Si:H/nc-Si:H layers. The 150 nm thick ITO layer was RF-sputtered from a ceramic target and 0.1 % oxygen in the Ar/O_2 sputter gas mixture. The 70 nm thick AZO layer was sputtered under DC conditions (ZnO:Al target with 1 % doping and 0.35 % oxygen in the Ar/O_2 sputter gas mixture), as well as the subsequent Ag metallization with a thickness of 800 nm. For the ITO wafer, the sputtered Ag was thickened by thermal evaporation (final thickness ~2 µm). For the Al wafer, a 1.5 µm thick aluminum layer was directly thermally evaporated onto the a-Si:H layers. The Al wafer was annealed at 150 °C for 30 minutes and subsequently at 160 °C for another 8 minutes. The ITO wafer was annealed at 200 °C for 15 minutes and at 210 °C for 20 minutes. The AZO wafer was annealed at 190 °C for 20 minutes followed by another 5 minutes at 210 °C (see Table 1).

Table 1. Process parameters

Backend	TCO thickness (nm)	Me thickness (nm)	ARC	Annealing
ITO/Ag	150	2000	(i)a-Si:H/SiN_X	200°C/15 Min + 210°C/20 Min
Al	/	1500	2*SiN_X	150°C/30 Min + 160°C/8 Min
AZO/Ag	70	800	(i)a-Si:H/SiN_X	190°C/20 Min + 210°C/5 Min

All layers were structured by photolithography. Etching the doped layers always entails etching the underlying intrinsic layers as well, making a repassivation necessary. To ensure passivation across the whole wafer, the n-type BSF structure overlaps the p-type emitter with a 15 µm margin. The p-type emitter layer (deposited first) was etched with an acidic solution, the n-type BSF layer with an alkaline solution. The latter etches intrinsic and n-type a-Si:H/nc-Si:H at a much faster rate than any p-type material, thus leaving the underlying and already structured emitter layer practically unharmed during the BSF patterning. The total metallization gap amounts to 30 µm. The cell area is 1 cm^2, not including the bus bars (designated area).

JV characteristics of all solar cells were measured with a Wacom WXS-156S-L2, AM1.5GMM dual source (tungsten and xenon lamp) sun simulator with class AAA characteristics. During the measurement, the solar cells are placed into a water-cooled chuck and thus kept at a temperature of 25°C. Suns-V_{OC} and lifetime (Quasi-Steady-State-Photoconductance – QSSPC) measurements were carried out at room temperature, using a WCT-100 photoconductance tool by Sinton Consulting Inc for the latter. Reflection spectra were recorded using a Perkin-Elmer LAMBDA 1050 UV/Vis/NIR Spectrophotometer. EQE measurements were performed on two self-made systems, with the first having a spot size of 2 by 4 mm and the latter having a large spot size greater than the actual cell area (cells were measured with proper shadow masks). Both systems were calibrated with a reference cell and white bias light was applied during measurements. The small spot system (EQE1) features a better grating for the wavelength range up to 460 nm, while the large spot system's (EQE2) overall accuracy is better due to irradiating the whole cell area. The final EQE curves were constructed by merging the data from EQE1 from 300 to 460 nm and EQE2 from 460 nm onwards.

3. Results and discussion

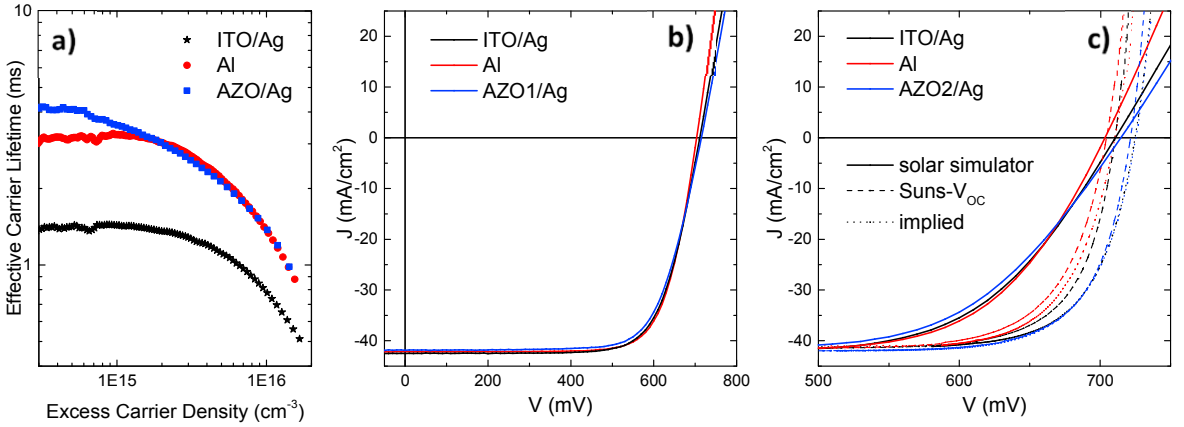

Fig. 1. (a) minority carrier life time curves measured after repassivation for all three cell types (b) 1-sun JV curves of the best cells (c) 1-sun JV, Suns-V_{OC} and implied JV curves for all cell types – note the different scale of the abscissa in (b) and (c).

In Figure 1a the minority carrier lifetime vs. excess carrier density after repassivation is depicted for all three configurations. Figure 1b shows the best cells' JV curves under 1 sun illumination, in Figure 1c the Suns-V_{OC} and implied JV curves are added (in Figure 1b and 1c the AZO cells differ). The ITO- and the AZO-wafers were processed in a different PECVD chamber using a more optimized process including an intrinsic a-Si:H passivation

layer at the front side, thus significantly higher lifetimes than for the Al wafer are measured. Table 2 summarizes all the relevant cell parameters. The lower lifetime of the Al wafer is reflected in a lower V_{OC} compared to the ITO and the AZO cell. To determine the fill factor potential, the lifetime data is used to calculate an implied fill factor (iFF) indicating an upper boundary [5]. Since mainly the shape of the lifetime curve determines the implied FF, all three wafers achieve similar values. The actual FF strongly deviates from the implied FF. To identify the origin of the drastic difference between the FF extracted from the JV data and the implied FF, the pseudo-FF (pFF) is determined by Suns-V_{OC} measurements. In all three cases, the pFF is very close to the iFF indicating that there are almost no non-ohmic FF losses. The difference between the measured FF and the pFF can be attributed to the series resistance of the corresponding solar cells. This difference exceeds 10 %abs for the ITO and AZO cell and, with 7 %abs, remains at a high level for the Al cell. In a previous publication [6], we have shown, that annealed aluminum can form a contact to amorphous silicon with a very low resistivity. Further annealing might increase the fill factor, but will also certainly diminish the solar cell's V_{OC}. This particular Al cell was therefore annealed to maximize the fill factor without decreasing the V_{OC}. The AZO cells achieve slightly lower FF values than their ITO counterpart, which is not surprising as AZO, being less conductive than ITO, is expected to form a marginally less efficient tunnel-recombination contact to p-type a-Si:H – overall the difference is negligible and therefore compensated by an advantage in V_{OC} and especially J_{SC}.

Table 2. Solar cell illuminated JV parameters

Metallization	V_{OC} (mV)	J_{SC} (mA/cm^2)	FF (%)	pFF (%)	iFF (%)	η (%)
ITO/Ag	711	41.5	73.1	83.4	83.5	21.6
Al	703	41.6	75.2	82.2	83.2	22.0
AZO1/Ag	715	41.9	72.2	/	83.6	21.6
AZO2/Ag	715	41.9	71.2	83.8	83.6	21.3

Since the AZO layers are both more transparent and thinner than the ITO ones in the reference, EQE measurements (Figure 2a) reveal a distinctive enhancement in the long wavelength range when AZO is used as the TCO material. Having a closer look on wavelengths greater than 1000 nm (Figure 2b), the Al cell suffers from worse reflection properties compared to its Ag counterparts, thus performing worst. The ITO cell slightly outperforms the Al one, as the 150 nm thick buffer layer also suppresses parasitic plasmonic absorption in the metal. The ITO is still fairly conductive ($n_{ITO} = 2*10^{20}$ cm^{-3}), possibly causing avoidable parasitic absorption. Increasing the thickness of the AZO buffer layer from 70 nm to around 150 nm might increase its capability to effectively suppress parasitic plasmonic absorption in the silver metallization [7].

The Al cell features a front side made of a double stack of SiN_X instead of an (i)a-Si:H passivation layer and a single SiN_X anti reflection coating. Having the better (front side) passivation, the ITO and the AZO cell's IQE is slightly higher in the medium wavelength range from 600 to 800 nm, as less recombination takes place close to the front side, where most of the incoming light is absorbed. Comparing the IQE curves of all three cells in the short wavelength range the difference between the Al curve and the ITO respectively the AZO curve (as they are almost identical) represents losses due to parasitic absorption in the front side amorphous silicon passivation layer. Furthermore, the SiN_X double layer of the Al cell shows significantly better antireflection properties in this wavelength range. Overall, however, these different effects cancel out, so that the J_{SC} values for the Al and the ITO cell extracted from the EQE measurements are almost identical (41.6 and 41.5 mA/cm^2). The advantage of AZO in the long wavelength range increases the J_{SC} of these cells by almost 0.5 mA/cm^2 compared to the two other cell types.

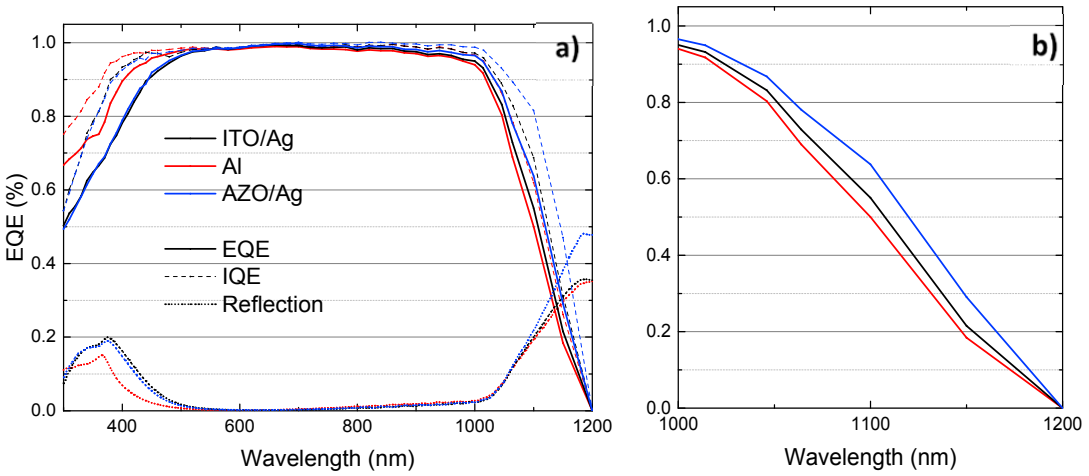

Fig. 2. (a) EQE, IQE and reflection spectra for all metallization variations; (b) EQE in the long wavelength range.

4. Conclusion

We have fabricated interdigitated back contact silicon heterojunction solar cells featuring either an ITO/Ag, an AZO/Ag or a simple Al back contact. In replacing ITO, both AZO and Al show certain benefits and drawbacks. The superior optical properties of the AZO layers grant these cells higher J_{SC} values, at the expense of slight resistive losses. The Al cells show the exact opposite behavior, as the series resistance substantially decreases and thus the FF increases. The low V_{OC} remains a problem for the Al cells, although this is likely not entirely related to the Al itself, but also to an initially worse passivation. Both approaches show potential for improvement: these particular AZO layers are not yet optimized for a back contacted architecture, and Al cells on wafers with a passivation quality equal to the ones used for the ITO and AZO cells were not yet built either.

Acknowledgements

This work was supported by the European Union's Horizon 2020 Programme for research, technological development and demonstration under grant agreement no. 727523 (project NextBase). Furthermore, the authors thank P. Wagner, H. Rhein, E. Conrad, M. Wittig, K. Jacob, M. Hartig, H. Kohlenberg, and T. Friedrich for their support in fabricating the solar cells.

References

[1] Richter, A., Hermle, M., Glunz, S. W., Reassessment of the limiting efficiency for crystalline silicon solar cells, IEEE J. Photovolt. 3(4), 013107, 2013

[2] Taguchi, M., Yano, A., Tohoda, S., Matsuyama, K., Nakamura, Y., Nishiwaki, T., Fujita, K., Maruyama, E., 24.7% Record Efficiency HIT Solar Cell on Thin Silicon Wafer, IEEE J. Photovolt. 4, 96–99 (2014).

[3] Yoshikawa, K., Kawasaki, H., Yoshida, W., Irie, T., Konishi, K., Nakano, K., Yamamoto, K., Silicon heterojunction solar cell with interdigitated back contacts for a photoconversion efficiency over 26 %. Nature Energy, 2(March), p.17032, 2017

[4] Morales-Vilches, A. B., Mazzarella, L., Hendrichs, M.-S., Korte, L., Schlatmann, R., Stannowski, B., Nanocrystalline vs. amorphous n-type silicon front surface field layers in silicon heterojunction solar cells: Role of thickness and oxygen content, 33rd EU-PVSEC, Amsterdam, to be published, 2017.

[5] Leilaeioun, M., Holman, Z. C., Accuracy of expressions for the fill factor of a solar cell in terms of open-circuit voltage and ideality factor, J. Appl. Phys. 20(12), p. 123111, 2016

[6] Stang, J.-C., Franssen, T., Haschke, J., Mews, M., Merkle, A., Peibst, R., Rech, B., Korte, L., Optimized Metallization for Interdigitated Back Contact Silicon Heterojunction Solar Cells, Sol. RRL, p.1700021, 2017

[7] Holman, Z. C., Filipič, M., Descoeudres, A., De Wolf, S., Smole, F., Topič, M., Ballif, C., Infrared light management in high-efficiency silicon heterojunction and rear-passivated solar cells, J. Appl. Phys., 113(1), p.13107, 2013